

# Structure and multiplicity of detonation regimes in heterogeneous hybrid mixtures

B. Veyssi re<sup>1</sup>, B.A. Khasainov<sup>2</sup>

<sup>1</sup>Laboratoire d'Energetique et de Detonique, U.R.A. C.N.R.S. 193, E.N.S.M.A. Poitiers, Site du Futuroscope, BP 109, F-86960 Futuroscope, France

<sup>2</sup>Institute of Chemical Physics, Russian Academy of Sciences, Moscow, Russian Federation

Received Nov. 16, 1993 / Accepted Dec. 9, 1993

**Abstract.** The problem of propagation of steady nonideal detonations in heterogeneous hybrid mixtures is studied in the case of a hydrogen-air gaseous mixture with suspended fine aluminum particles. Due to the difference in the order of magnitude of the characteristic induction and combustion times of gaseous mixture and solid particles, the process of energy release behind the leading shock front occurs over an extended period of time and in a nonmonotonic way. An approximate numerical model has been improved to find the steady propagation regimes and investigate their structure. The problem is analyzed in the frame of the theory of the mechanics of multiphase media with mass, momentum and heat exchanges between particles and gases. The one-dimensional ZND model of detonation with losses to the lateral boundaries is used. It is shown that three different steady propagation regimes may exist: the Pseudo-Gas Detonation (PGD), the Single-Front Detonation (SFD) and the Double-Front Detonation (DFD). The numerical results match the available experimental results obtained previously. The influence of the fundamental parameters of the system on the domains of existence of the different regimes is displayed. Moreover, it is shown that, according to the theory of nonideal detonations with nonmonotonic energy release, there may exist a multiplicity of detonation modes. However, the total number of solutions actually obtained by numerical calculations differs from that predicted by the theory. The reasons for these discrepancies are discussed.

**Key words:** Detonation, Solid particles, Hybrid mixtures

## 1. Introduction

Heterogeneous hybrid mixtures consist, for example, of reacting particles or droplets suspended in a gaseous combustible mixture. Those multi-phase mixtures are characterized by the fact that during a combustion process, heat release may be provided by different sources: for example, gaseous components and solid particles, or gaseous components and liquid droplets, etc... Due to the different nature

of the mixture components, the characteristic times of the mechanisms which govern the process of combustion (heat exchanges, diffusion, induction delay, reaction rate, etc...) may differ by important proportions, even by an order of magnitude or more. In the case of a detonation, there also may exist behind the detonation front various causes of heat losses from the flow, imposed, for example, by the walls which bound the explosive mixture. As a result, the actual process of energy release behind the leading front is generally nonmonotonic and occurs over a long time interval. This is often the case, of heterogeneous hybrid mixtures, since the characteristic time for combustion of solid particles to reach completion is far greater than the characteristic time of homogenous gaseous reactions. Thus, two-phase mixtures, beyond the fact that they are heterogeneous, may give rise to a nonmonotonic process of energy release. Such situations deviate strongly from the classical CJ model of ideal detonations. For this reason, detonative propagation regimes in these mixtures are often called "non-ideal detonations". Further studies are needed to elucidate what can be the propagation regimes for a detonation in such conditions and which structure they have.

The variety of detonation regimes which may propagate in hybrid, two-phase mixtures was demonstrated by Veyssi re and Manson (1982) and Veyssi re (1986) who observed the propagation of single-front detonations in suspensions of aluminum particles in gaseous explosives mixtures and have provided experimental evidence of the possibility of quasi-steady propagation of double-front detonations under certain experimental conditions. It is known also that low-velocity detonations can propagate in two-phase media: for example Saint-Cloud (1976) examined such low-velocity detonation regimes in mixtures of combustible gases with water foams and Mamontov et al. (1980) observed similar regimes in a  $C_2H_2+O_2$  mixture in a shock tube filled with inert particles of sand or steel. Of course, those two-phase mixtures are not hybrid, but low-velocity regimes of that kind may be considered as an extreme case of detonation propagation in hybrid mixtures when particles remain inert upstream of the CJ point. However, the experimental results available up to now, do not permit to correlate (even in

an empirical way) the observed propagation regimes to the intrinsic parameters of the explosive mixture.

Therefore, a model, even very simplified, is needed to be able to predict the detonation behavior in such a reactive system. The most attractive theoretical model is that proposed by Zel'dovich and Kompaneets (1960) and generalized for any arbitrary nonmonotonic heat release by Kuznetsov (1967 and 1968). It is based on the ZND scheme of detonation, which takes into account a finite rate of chemical reactions and allows one to compute in homogeneous media the detonation velocity deficit caused by losses of different kinds. This plane steady model predicts accurately the average detonation velocity for gaseous, liquid and condensed explosives in spite of the intrinsic multidimensional structure and the nonstationarity of detonation fronts. However in the case of gaseous systems, predicted CJ pressures and densities may exceed significantly (up to 15%) experimental values (Nettleton 1987). In spite of those discrepancies between experimental data and the ZND scheme, it was very useful in improving the knowledge about detonation mechanisms in different substances, including two-phase media (see for example the survey by Mitrofanov 1988). This model was also used to compute successfully detonation limits of many explosive substances. Hence, one can expect that a model based on the ZND scheme should provide useful results for the hybrid two-phase mixtures taking into account the fact that the energy release in these mixtures generally is nonmonotonic and occurs in, at least, two steps.

In the present paper, we expose the approximate numerical model which we have improved to analyze the characteristics and structure of steady, plane, non-ideal detonation regimes in hybrid two-phase mixtures, and discuss the results obtained with this model. Here, we do not treat the fine structure of the detonation front since, at the present stage, we are primarily interested by the profiles of flow parameters between the shock front and the CJ point of the detonation wave. First, we discuss the particular features of the process of energy release in the case of hybrid detonations. Then, we present the basics of the non-ideal detonation modeling and the method used to get steady solutions. Investigation of the different detonation regimes is made by analysis of the integral paths. Details of the structure of those regimes and their dependence on the fundamental parameters of the system are provided. At last, the problem of the existence of multiple detonation modes is examined and our particular numerical results are discussed in reference to the theoretical predictions of the general theory of non-ideal detonations of Kuznetsov. We think that this simplified approach of a very complex problem will be able to provide a map of the range of phenomena which can occur and is one step toward achieving a better knowledge in view to perform unsteady, multidimensional direct simulations of hybrid mixture detonations.

## 2. The process of energy release in the case of hybrid detonations

Here, we focus our attention on gaseous combustible mixtures with suspended reactive particles. This situation may be met in the so-called "dusty mixtures". As it is shown

hereafter, important information may be obtained from the analysis of this particular case in the frame of the steady plane ZND model. But we believe that we have not restricted the validity of our investigation by studying this particular problem, and that some of our results may lighten the understanding of the more general problem of the detonation behavior when energy release is nonmonotonic.

Let us consider a reactive gaseous mixture in which a steady detonation can propagate. Let us suppose that solid reactive particles are uniformly dispersed in this mixture. These solid particles can react with the gaseous components or with the products of the gaseous reactions. The dusty mixture is contained in a detonation tube with rigid walls, so that friction and heat losses to the tube walls in the flow downstream of the leading detonation front must be taken into account. As pointed out above, the process of energy release in such a system is very complicated and depends on a great number of parameters of the system. For going on further in the analysis of this problem, a very simple kinetics model is sufficient, which does not restrain the validity of our reasoning. A global, two-step reaction scheme is assumed for homogeneous gaseous reactions: the first step describes an induction time, the second one corresponds to the reaction time (Korobeinikov et al. 1972); the second time is much more smaller than the first one. For the solid particles, a criterion is chosen for achieving ignition at a prescribed temperature: before this temperature is reached, particles are regarded as chemically inert; beyond the ignition temperature, the burning of particles is modeled by a global empirical kinetic law. Thus, with such a simplified modeling, the induction and combustion processes of gases and particles are treated nearly in a similar manner, and there is a possibility of varying the characteristic time scale of each process over a large range. In many cases, ignition of particles occurs after the end of gaseous reactions (see below), but it is not a necessary condition.

A relevant parameter of energy evolution behind the shock front is the effective energy release rate  $dq/dt = dq_+/dt - dq_-/dt$ , which is the balance at time  $t$  between the energy release rate from chemical reactions and the energy loss rate due to the different sinks of energy losses. If we consider the case of an ignition of solid particles after the end of gaseous reactions, the energy release evolution will be typically as follows (see Fig. 1):  $dq/dt$  is, first, negative in the gaseous induction zone behind the leading shock front, due to the effect of energy losses to the inert particles and the walls. After the beginning of gaseous reactions,  $dq/dt$  increases, goes through zero and becomes positive. At the end of gaseous reactions, the heat loss rate become again predominant, inducing a decrease of the effective energy release rate. As a consequence,  $dq/dt$  goes through zero and becomes negative. Re-augmentation of the effective energy release rate will be obtained after the ignition of solid particles, leading to a new change of sign of  $dq/dt$ , which becomes again positive. Then,  $dq/dt$  undergoes a new maximum and decreases to negative values, due to the effect of energy losses. As a result, energy release profile  $q(t)$  behind the shock passes through two maxima separated in time and space.

The steady propagation of a non ideal detonation is insured by fulfilling the so-called equivalent CJ condition

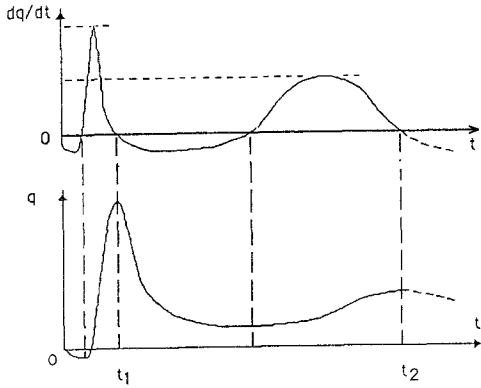


Fig. 1. Scheme of heat release evolution behind the detonation front of a heterogeneous hybrid mixture

(Zel'dovich and Kompaneets 1960), which requires that two conditions must be satisfied simultaneously in a certain point of the flow downstream of the leading shock: the local Mach number ( $M = (D - u)/c$ ) must be equal to unity  $M = 1$ , and the effective energy release rate to zero:  $dq/dt = 0$  (stable regimes correspond to a local maximum of energy release (Zel'dovich and Kompaneets 1960; Kuznetsov 1967 1968), that is  $d^2q/dt^2 < 0$  at the sonic point). Thus, the existence and structure of steady non-ideal detonation waves is determined by the possibility to achieve or not the sonic condition at the points of the flow where  $dq/dt = 0$ . If we refer to the above example, steady regimes can be obtained if the sonic condition is achieved either at the second or at the fourth crossing of  $dq/dt$  through zero, which correspond to local maxima of energy release. Due to the competition between energy release and loss rates upstream of the sonic locus, this equivalent CJ condition predicts a detonation velocity deficit as compared with the value of the velocity of the ideal detonation (without losses), the magnitude of this deficit is determined by the actual process. Moreover, chemical reactions may be not complete at the CJ point, and some part of the chemical energy be released downstream of the CJ point.

### 3. The modeling of detonation in the hybrid two-phase mixtures

The model improved to investigate quantitatively the detonation process in hybrid mixtures has been described in details elsewhere (Veyssi re and Khasainov 1991). It treats the steady propagation of plane, one-dimensional, non-ideal detonations in a mixture of gaseous explosive with reactive solid particles. The particles are assumed incompressible, not interacting between one another and their volume fraction in the whole mixture is negligible. Moreover, we neglect the temperature gradients inside the particles: in our case, it can be verified that the characteristic time for conduction heat transfer inside a particle is negligible as compared with other characteristic times, for particle diameters  $< 50 \mu\text{m}$ . For larger particles, an approach like that proposed by Fan and Sichel (1988) to take account of heat conduction inside the particles can be used to refine the model. Mainly,

it will modify slightly the value of the ignition delay, but will not affect the nonmonotonic nature of energy release which is responsible of the effects studied here. Thus, the choice of a unique temperature for particles does not constrain the validity of our reasoning and the generality of our conclusions.

The usual assumptions of the theory of multi-phase flows (Nigmatulin 1987) are used: velocities and temperatures are assumed to be different for particles and gases; mass, momentum and heat exchanges between particles and gases are taken into account. The detonation is described following the ZND model (Zel'dovich and Kompaneets 1960), i.e., a shock thermally initiating chemical reactions, but with viscous and thermal losses to the tube walls allowed behind the shock wave (they are treated in a quasi-one dimensional approximation). From these assumptions, follows the time-independent set of Euler equations written in coordinates linked to the leading front:

#### Solid particles

Balance equations:

Mass:

$$\frac{d}{dz}(\sigma_{p_i} v_{p_i}) = -J_i \quad i = 1, \dots, N \quad (1)$$

Momentum:

$$\frac{d}{dz}(\sigma_{p_i} v_{p_i}^2) = f_i - J_i v_{p_i} \quad i = 1, \dots, N \quad (2)$$

Energy:

$$\frac{d}{dz}(\sigma_{p_i} v_{p_i} e_{p_i}) = q_i - J_i e_{p_i} \quad i = 1, \dots, N \quad (3)$$

$$\text{with } e_{p_i} = C_p T_{p_i} + Q_{A_i} \quad (4)$$

$i = 1, \dots, N$  correspond to different fractions of particles of discrete diameter

$\sigma_{p_i}$  mass concentration of the  $i$ -th fraction of particles

$v_{p_i}$  velocity of the  $i$ -th fraction of particles

$J_i$  mass exchanges between particles and gases

$f_i$  momentum exchanges between particles and gases

$q_i$  heat exchanges between particles and gases

$e_{p_i}$  internal energy of particles

$C_p$  heat capacity of particles

$T_{p_i}$  temperature of the  $i$ -th fraction of particles

$Q_{A_i}$  effective heat effect of the global reaction between particles and oxidizing gases (see Veyssi re and Khasainov 1991a)

Conservation of the number of particles:

$$\frac{d}{dz}(N_{p_i} v_{p_i}) = 0 \quad i = 1, \dots, N \quad (5)$$

Gaseous phase

Balance equations:

Mass:

$$\frac{d}{dz}(\rho_g v_g) = \sum_{i=1}^N J_i \quad (6)$$

Momentum:

$$\frac{d}{dz}(p + \rho_g v_g^2) = \sum_{i=1}^N (J_i v_{p_i} - f_i) + 4 \frac{\tau_w}{D_w} \quad (7)$$

Energy:

$$\begin{aligned} \frac{d}{dz} \left[ \rho_g v_g \left( \frac{\gamma}{\gamma - 1} \frac{P}{\rho_g} + \frac{v_g^2}{2} \right) \right] \\ = Q_{\text{gas}} + \sum_{i=1}^N \left[ J_i \left( e_{p_i} + \frac{v_{p_i}^2}{2} \right) - f_i v_{p_i} - q_i \right] \\ + 4 \frac{\tau_w}{D_w} D_{\text{CJ}} - 4 \frac{q_w}{D_w} \end{aligned} \quad (8)$$

$$\gamma = c_p / c_v$$

$\rho_g, v_g$  density and velocity of gases

$\tau_w$  viscous stress to the walls

$q_w$  heat flux to the walls

$D_{\text{CJ}}$  detonation velocity

$D_w$  hydraulic diameter of the tube

$Q_{\text{gas}}$  heat release from gaseous reactions

For modeling the gaseous reactions, the two-step scheme (an induction zone followed by a reaction zone) of Koro-beinikov et al. (1972) has been chosen. Hence, after the beginning of the reactions:  $Q_{\text{gas}} = \rho_g Q_g \frac{d\beta}{dz}$

$Q_g$  thermal effect of gaseous reactions

$\beta$  fraction of decomposed gaseous explosive ( $\beta = 0$  during induction period)

*Interactions between solid particles and gases*

Mass exchange:

$$J_i = \begin{cases} 0, & T_{p_i} < T_{\text{ign}} \\ 3\sigma_{p_i} \left( \frac{\dot{d}}{d} \right)_i, & T_{p_i} \geq T_{\text{ign}} \end{cases} \quad i = 1, \dots, N \quad (9)$$

$T_{\text{ign}}$  ignition temperature of the particle

An empirical burning law (Price 1984) is chosen to model the regression rate of aluminum particles:

$$\left( \frac{\dot{d}}{d} \right)_i = -\frac{1}{t_{p_i}} \quad (10)$$

$$t_{p_i} = K d_{p_{oi}}^n / \phi^{0.9} \quad (11)$$

$d_{p_{oi}}$  initial value of the particle diameter for the  $i^{\text{th}}$  fraction

$\phi$  volume fraction of oxidizing species ( $\text{O}_2, \text{H}_2\text{O}$  and  $\text{CO}_2$ )

$K, n$  empirical constants of the burning law of an aluminum particle

$t_{p_i}$  burning time of a particle

Momentum exchange:

$$f_i = \frac{3}{4} \frac{\rho_g}{\rho_p} \frac{\sigma_{p_i}}{d_{p_i}} C_{d_i} (v_g - v_{p_i}) |v_g - v_{p_i}| \quad (12)$$

$\rho_g$  is the density of particles

with

Particle drag coefficient:

$$C_{d_i} = \frac{24}{\text{Re}_i} + \frac{4.4}{(\text{Re}_i)^{0.5}} + 0.42 \quad (13)$$

Reynolds number of the particle of the  $i$ -th fraction:

$$\text{Re}_i = \frac{\rho_g d_{p_i} |v_g - v_{p_i}|}{\mu_g} \quad (14)$$

is the gas viscosity.

Heat exchange:

$$q_i = \frac{6\sigma_{p_i}}{\rho_p d_{p_i}} \left[ \frac{\text{Nu}_i \lambda_g (T_g - T_{p_i})}{d_{p_i}} + \varepsilon \sigma_{\text{Boltz}} (T_g^4 - T_{p_i}^4) \right] \quad (15)$$

with,

$\sigma_{\text{Boltz}}$  Boltzmann constant

$\text{Nu}_i$  Nusselt number for the particle of the  $i$ -th fraction

$$\text{Nu}_i = 2 + 0.6 \text{Re}_i^{0.5} \left( \frac{c_{pg} \mu_g}{\lambda_g} \right)^{1/3} \quad (16)$$

$\lambda_g$  gas heat conductivity,

$c_{pg}$  gas heat capacity at constant pressure.

*Losses to the walls:*

$$\tau_w = \frac{\lambda_w}{8} \rho_g (D_{\text{CJ}} - v_g)^2 \quad (17)$$

$$q_w = \frac{\lambda_w}{8} \rho_g (D_{\text{CJ}} - v_g) c_{pg} (T_g - T_0) \quad (18)$$

$\lambda_w$  wall friction coefficient.

*Equation of state for gaseous products:*

$$\rho = \rho_g \bar{R} T_g \quad (19)$$

#### 4. The method of solution

By substituting the variable  $t$  in the equations ( $t$  is the time along the gas trajectory behind the front:  $d/dz = 1/v_g \cdot d/dt$ ;  $t = 0$  at the shock front), the above set of equations reduces to a system of ordinary differential equations:

$$\frac{dP}{dt} = -(\gamma - 1) M^2 \frac{dq_{\text{eff}}/dt}{1 - M^2} \quad (20)$$

$$\frac{dv_g}{dt} = \frac{1}{\rho_g} \left\{ -\frac{dP}{v_g dt} + \frac{4\tau_w}{D_w} + \sum_{i=1}^N [J_i (v_{p_i} - v_g) - f_i] \right\} \quad (21)$$

$$\frac{d\rho_g}{dt} = -\rho_g \frac{dv_g}{v_g dt} + \sum_{i=1}^N J_i \quad (22)$$

$$\frac{dv_{p_i}}{dt} = \frac{f_i}{\sigma_i v_{p_i}} \quad (23)$$

$$\frac{d\sigma_i}{dt} = -\frac{J_i + f_{p_i}/v_{p_i}}{v_{p_i}} \quad (24)$$

$$\frac{de_{p_i}}{dt} = \frac{q_i}{\sigma_i v_{p_i}} \quad (25)$$

$$\frac{dN_{p_i}}{dt} = -\frac{N_{p_i}}{v_{p_i}} \frac{dv_{p_i}}{dt} \quad (26)$$

$$\text{where } \frac{dq_{\text{eff}}}{dt} = \frac{dq_+}{dt} - \frac{dq_-}{dt} \quad (27)$$

with  $dq_+/dt$  the rate of energy release:

$$\frac{dq_+}{dt} = \rho_g Q_g \frac{d\beta}{dt} + Q_{\text{Al}} \sum_{i=1}^N J_i \quad (28)$$

and  $dq_-/dt$  the rate of energy losses:

$$\begin{aligned} \frac{dq_-}{dt} = & \frac{4q_w}{D_w} + \frac{4\tau_w}{D_w} \left[ \left( 1 + \frac{1}{(\gamma-1)M^2} \right) v_g - D_{\text{CJ}} \right] \\ & + \sum_{i=1}^N f_i \left[ v_{pi} - \left( 1 + \frac{1}{(\gamma-1)M^2} \right) v_g \right] \\ & - \sum_{i=1}^N J_i \left[ C_p T_{pi} + \left( \frac{v_{pi} - v_g}{2} \right)^2 - \frac{v_g}{(\gamma-1)M^2} (v_{pi} - v_g) \right] \end{aligned} \quad (29)$$

$M = v_g/a_g$  is the local Mach number ( $v_g$  is the gas phase velocity relative to the shock front,  $a_g = (\gamma p_g/\rho_g)^{1/2}$ ); just behind the shock front  $M < 1$ .

The behavior of this system may be derived from the examination of the equation for pressure rate (20), which is the most convenient parameter for comparison with experiments. It is of interest, for the future discussion in the next sections of the paper, to note that a reliable estimation of the energy release rate (after completion of gaseous reactions) is provided by the approximate relationship:

$$dq_+/dt \approx \sigma_{p_0} Q_{\text{Al}} \phi^{0.9} / d_{p_0}^2 \quad (30)$$

with  $\sigma = \sigma_{p_0}$ , the initial particle concentration of the fresh mixture and  $d_{p_0}$ , the mean diameter of the particles.

According to the theory of nonideal detonations (Zel'dovich and Kompaneets 1960), the detonation velocity should be selected so that the equivalent CJ condition:

$$dq_+/dt = dq_-/dt \quad \text{and} \quad M = 1 \quad (31)$$

be satisfied in a point of the flow at the rear of the leading front, that is the equation of the pressure rate has a peculiar saddle point.

Due to the complexity of the problem (two phases with two velocities and two temperatures), the system of governing ordinary differential equations cannot be solved analytically, and the solution is derived numerically. For this purpose, we have used a Gear algorithm (Gear 1971), which permits to treat satisfactorily the "stiff" behavior of the Arrhenius law describing the gas-phase chemical reactions.

To determine the value of the CJ detonation velocity  $D_{\text{CJ}}$ , which is an eigenvalue of the problem, a try and error technique has been used, i.e. the value of the detonation velocity is varied to obtain the convergence of the different integral paths to a saddle point satisfying Eq.(31). The saddle point is located on a separatrix which determines two families of curves: for  $D = D_{\text{ov}} > D_{\text{CJ}}$ , the integral curve beginning at the shock front, at  $M < 1$ , will meet primarily either the first, or second, or further appearance of the condition  $dq_+/dt = dq_-/dt$  this wave may propagate steadily only if it is supported by a piston, which is the overdriven

case. For  $D = D_{\text{ch}} < D_{\text{CJ}}$ , the integral curve beginning at the shock front will meet first, the condition  $M = 1$ ; the solution ends in the sonic point with infinite gradient, which corresponds to the choking case. For the stable detonation wave  $D_{\text{ch}} < D_{\text{ov}}$  (Zel'dovich and Kompaneets 1960).

Iterations are done until the difference between  $D_{\text{ov}}$  and  $D_{\text{ch}}$  becomes less than a prescribed value. In the single-front detonation problem (see below Sect. 5), it is sufficient in most cases to limit the accuracy to 0.1 m/s. In the double-front detonation problem (see Sect. 5), the iterations around the first CJ point are done till the exact pass of the integral curve through the saddle point and then, a second discontinuity front having the same velocity  $D_{\text{CJ}}$  is set at a given delay after the leading front (see Khasainov and Veyssi re 1987). The position of this secondary detonation front is defined by iterations with some accuracy (say 2.5  $\mu\text{sec}$ ), so that to satisfy again the CJ condition (31) a second time in the flow. To limit the time of computations, the parameters at this second CJ point were usually defined by extrapolation procedure (for the  $j^{\text{th}}$  trial, corresponding to the shock velocity  $D_j$ , the integration results at  $z_j$  either in  $M_j^2 = 1$  with a finite value of  $(dq_{\text{eff}}/dt)_j$ , or  $(dq_{\text{eff}}/dt)_j = 0$  with a finite value of  $(1 - M_j^2)_j$ ; having an array of non-zero values of  $(1 - M_j^2)_j$  and of  $(dq_{\text{eff}}/dt)_j$ , it is possible to define  $z_{\text{CJ}}$  by extrapolation to a zero value of  $(1 - M^2)$  or of  $(dq_{\text{eff}}/dz)$ , which permits to derive the corresponding CJ flow parameters; this approximation of the second CJ point is sufficient in most cases). Thus, it is possible to determine the structure of the steady single- or double-front detonation wave, i.e. the profiles of all the parameters in the zone between the leading shock front and final CJ point.

## 5. Typical integral paths

Let us begin the analysis of the flow structure from the treatment of different integral paths. This will help us to understand the existence of different detonation solutions and the characteristic features of different detonation regimes, namely: single-front (SFD), pseudo-gas (PGD) and double-front detonations (DFD). For this purpose, let us consider the results of computations obtained for a gaseous explosive mixture of hydrogen and air ( $\text{H}_2 + 0.47 \text{O}_2 + 1.77 \text{N}_2$ ) with an equivalent ratio 1.06. The other input parameters of the model have been described earlier (Khasainov and Veyssi re 1987, 1989a; Veyssi re and Khasainov 1991a). Let us recall only that the detonation tube has an internal diameter of 69 mm and a "technical" roughness 15  $\mu\text{m}$ ; the diameter of aluminum particles is set to 13  $\mu\text{m}$ . These values match the experimental conditions of Veyssi re (1986).

Let us examine, in a first time, the behavior of the integral paths of pressure just behind the shock front, for different shock front velocities (Fig. 2). According to Zel'dovich and Kompaneets (1960), pressure in the induction zone slightly grows due to losses to tube walls and particles (see Eq. 20). This increase is quite small because induction time of gaseous reactions is relatively short. Subsequent sharp decrease of pressure follows immediately after the beginning of fast exothermic reactions: thus, the condition  $dq_+/dt = dq_-/dt$  is fulfilled for the first time: this point

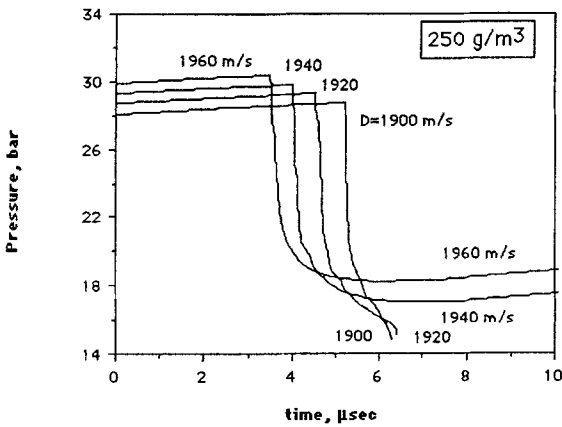


Fig. 2. Integral paths of pressure for pseudo-gas detonation solution at particle concentration  $\sigma = 250 \text{ g/m}^3$

corresponds to a minimum of energy release  $q(t)$  and to a maximum of pressure ( $M$  is still  $< 1$ ). Up to this stage of the process, the different integral curves do not differ qualitatively. On the opposite, after this change, the two integral paths with the largest velocities ( $D_{ov} = 1940$  and  $1960 \text{ m/s}$ ) correspond to the overdriven case: the condition  $dq_+/dt = dq_-/dt$  is satisfied again at the point where pressure passes through a minimum, and then, according to Eq. (20) pressure begins to grow again because energy losses rate prevail over energy release rate. On the opposite, the two other integral curves ( $D_{ch} = 1900$  and  $1920 \text{ m/s}$ ) result in choking: these curves begin with  $M < 1$ , at the shock front (at  $t = 0$ ) and end with an infinite gradient at the sonic point with  $dq_+/dt$  still greater than  $dq_-/dt$ . This behavior shows the existence of a peculiar point of saddle type. Further iterations allow one to diminish the difference between  $D_{ov}$  and  $D_{ch}$  and to compute the CJ velocity of nonideal detonation, which results here in the value  $D_{CJ} = 1926.111 \text{ m/s}$ . Following the conditions (31), the heat release  $q(t)$  at this CJ point reaches a maximum value.

The arrangement of the integral curves in this simple and well-known example allows, according to Zel'dovich and Kompaneets (1960), to conclude that this solution is stable to the effect of infinitely small perturbations. Indeed, the overdriven wave with  $D_{ov} > D_{CJ}$  may propagate steadily under the only condition that this wave is supported by a piston, otherwise it must decelerate. On the opposite, if a perturbation decreases the velocity of a wave front  $D_{CJ}$  to  $D_{ch} < D_{CJ}$ , the wave must accelerate due to chemical reaction. This conclusion about structural stability of the ZND detonation wave does not contradict the experimental evidence of hydrodynamic inherent instability and multidimensional structure of real detonation waves, which nevertheless travel with an average velocity very close to the CJ detonation velocity if losses are relatively small.

Because particles do not ignite upstream of the CJ point of the detonation wave shown in Fig. 2, this simple regime is called "pseudo-gas" detonation wave (PGD): aluminum particles remain inert and do not contribute to support the detonation propagation by releasing their chemical energy. In

this case, the combustion of particles takes place downstream of the CJ point, generally in the unsteady expansion wave which cannot be analyzed in the frame of the steady model. However, this steady model can predict the existence (or absence) of other steady self-sustained single- or double-front detonations which may be due to burning of aluminum.

For example, Figs. 3–5 show the profiles of pressure, Mach number (squared) and dimensionless effective energy release behind the shock front  $Q(t) = K \cdot (q_+ - q_-)$  (at  $t = 0$ ,  $Q = 0$ ), in the same conditions as on Fig. 2, but for velocities exceeding or equal to the PGD detonation velocity  $D = 1926.111 \text{ m/s}$  (at smaller  $D$  choking takes place, as was demonstrated earlier). Shock wave velocities are indicated near the corresponding profiles. Continuation of steady profiles corresponding to  $D = 1926.111 \text{ m/s}$  from subsonic to supersonic zone at  $t > t_{CJ} \approx 8 \mu\text{s}$  are also shown (see in Figs. 3–5 dashed curves marked by letter [A]; but, due to the fact that gaseous reactions are much faster than the burning of aluminum particles, the part of the flow which is controlled by gaseous explosive decomposition occupies about  $8 \mu\text{s}$  and, thus, is not well resolved in Figs. 3–5). These curves represent one of two separatrices passing through the saddle CJ point at  $t = t_{CJ}$ , the other separatrix is marked as [B] on Figs. 3–5.

Examination of the flow pattern on Figs. 3–5 indicates that there exists another solution, different from the PGD solution (with  $D_{CJ} = 1926.111 \text{ m/s}$ ), and the velocity of which is between  $D_{ch} = 1950$  and  $D_{ov} = 1960 \text{ m/s}$ ; successive iterations lead to the value  $D_{CJ} = 1951.70 \text{ m/s}$ . This solution corresponds to single-front detonation (SFD), i.e. it is supported by reactions of gas and aluminum. The integral path corresponding to  $D = D_{ch} = 1940 \text{ m/s}$ , which was one of overdriven solutions in the PGD case (Fig. 2), now results in choking but at much larger times ( $M = 1$  at about  $700 \mu\text{s}$ ). The curve obtained for  $D = 1960 \text{ m/s}$  corresponds again to an overdriven solution. Ignition of aluminum particles takes place before the maximum of pressure, which is reached at about  $t = 150 \mu\text{s}$  (Fig. 3). Then,  $dq_+/dt$  grows, due to energy release from particles, and becomes greater than energy losses rate  $dq_-/dt$ . As a result, pressure begins to drop. Note that the behavior of Mach squared profiles (Fig. 4) is opposite to that of pressure profiles. The behavior of energy release (Fig. 5) is quite complicated because it is governed not only by nonmonotonic chemical heat release from different reactions but also by all kinds of losses. Nevertheless, just after the shock front, energy is, at first, absorbed from gas to tube walls and particles so that  $q$  is negative just behind the shock front as was mentioned above. This stage is followed by fast release of gas chemical energy and  $q$  reaches the first maximum (see Fig. 5). Then, energy is transferred from gas to particles (they are not only heated, but also accelerated by gas) and after ignition of particles, heat is again released in the gas phase. At the CJ point of SFD, energy release reaches the second local maximum according to Eq. (31).

The shape of pressure profiles in the case of SFD (Fig. 3) at the vicinity of CJ point (at  $t = 900 \mu\text{s}$ ) shows that SFD, as well as PGD, is structurally stable. Consideration of smooth evolution of integral paths on Fig. 2 and Figs. 3–5 at different values of the velocity  $D$ , indicates that there does not exist any intermediate unstable solution with a

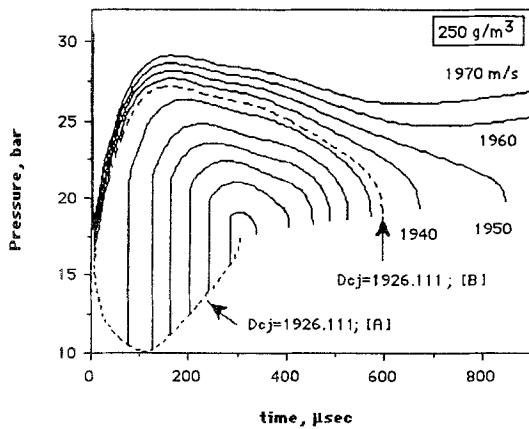


Fig. 3. Integral paths of pressure at particle concentration  $\sigma = 250 \text{ g/m}^3$

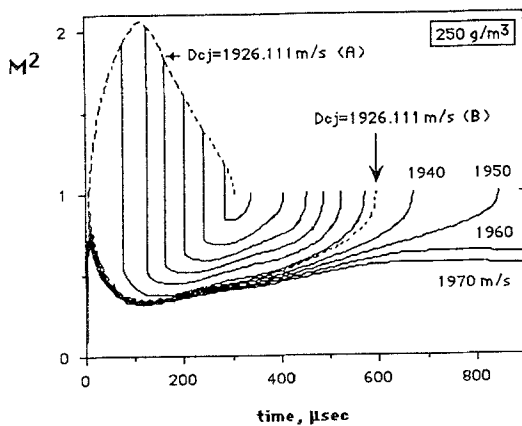


Fig. 4. Integral paths of Mach number (squared) at  $\sigma = 250 \text{ g/m}^3$

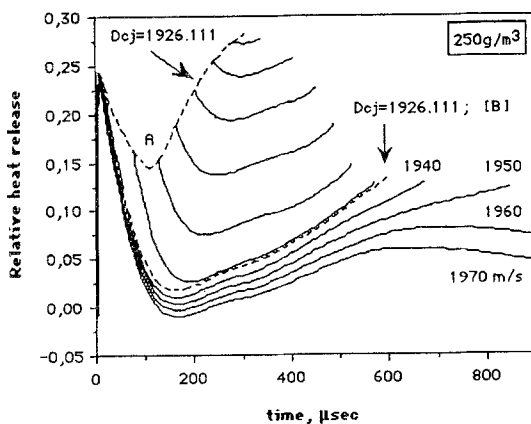


Fig. 5. Profiles of relative heat release behind the shock front at particle concentration  $\sigma = 250 \text{ g/m}^3$

detonation velocity between  $D_{\text{PGD}}$  and  $D_{\text{SFD}}$ , as could be expected from theoretical predictions by Kuznetsov (1967, 1968). This point will be discussed later.

Let us now examine the region between the two separatrices shown on Fig. 3–5 by dashed lines. It is worthy to

note that between choking points of the two separatrices corresponding to  $D_{\text{PGD}} = 1926.111 \text{ m/s}$  there is a large “gap”, which appears to be “forbidden” for integral curves (see Fig. 3, where  $t_{\text{ch}} = 305 \mu\text{s}$  for separatrix A and  $\approx 600 \mu\text{s}$  separatrix B). Let us consider in more details the behavior of the integral curves of Figs. 3–5 which correspond to the PGD wave, but in the region downstream of the first CJ point, i.e. at  $t > 8 \mu\text{s}$ : the flow may follow one of the two separatrices, either A or B. Along the branch B, the flow remains subsonic up to the choking point at  $600 \mu\text{s}$  and hence, this continuation cannot be matched with supersonic flow in the rarefaction wave; thus branch B has no practical interest because there is no way for the detonation products to reach supersonic velocity. Let us consider now the branch A. In contrast to integral paths with  $D > D_{\text{PGD}} = 1926.111 \text{ m/s}$  which everywhere, except choking points, are subsonic, this integral curve with  $D = D_{\text{PGD}}$  after it leaves the CJ point of PGD (at  $t > 8 \mu\text{s}$ ), becomes supersonic and this is why burning of aluminum particles is accompanied by pressure increase and drop of Mach number, and finally  $M$  becomes equal to unity at the choking point (at  $t = 305 \mu\text{s}$ ). Because continuous transition from supersonic (in the frame fixed to the detonation front) to subsonic flow is impossible and detonation products must have supersonic velocity downstream of the CJ point, the only possibility for the detonation products to satisfy to this requirement is to pass through a new shock. Figs. 3–5 show the set of integral curves which one obtains by locating a secondary shock at different positions downstream of the CJ point of PGD. The integral paths behind the secondary shock fronts exactly hit the gap between choking points of separatrices A and B. However, all those curves result in choking and, hence, steady double-front structure is impossible in the considered example: for this value of particle concentration, in the actual process the secondary detonation wave after its origination should overtake the leading PGD wave and increase its velocity to that of  $D_{\text{SFD}}$ , because there is no any other steady solution in this case.

Steady double-front detonation solution may be found in the same gaseous mixture, but at smaller particle concentrations, for example  $\sigma = 100 \text{ g/m}^3$  (Figs. 6–8). In this case, one easily finds the PGD solution, with  $D_{\text{PGD}} = 1962.062 \text{ m/s}$ , but SFD does not exist in this case: the integral curves with smaller velocity end at much smaller time with choking, whereas at even slightly larger velocities integral curves always result in the overdriven case. Hence, at this particle concentration only one steady PGD regime exists (it may be understood by taking into consideration the proportionality of  $dq_+/dt$  with the particle concentration  $\sigma$ , as displayed by the relation (30): below some critical value of  $\sigma$  the energy release rate is insufficient to allow existence of SFD). The separatrices passing through the CJ point of PGD are shown by dashed lines and again are marked as A and B. Pressure along the integral curve B passes now through a secondary minimum at  $t \approx 400 \mu\text{s}$  and choking does not take place at all. Such detonation wave may propagate steadily under the only condition that it is supported by a piston. The other separatrix A, after ignition and burning of aluminum particles, meets the choking condition. Hence, following the same reasoning as above, one should try to find a solution with a secondary shock separated by a time delay  $\tau_{\text{CJ}}$  from the first

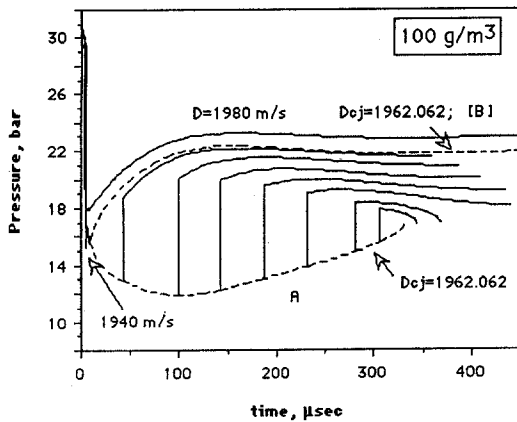


Fig. 6. Integral paths of pressure at particle concentration  $\sigma = 100 \text{ g/m}^3$

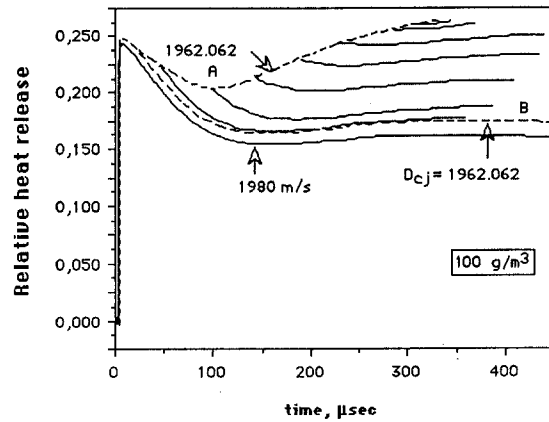


Fig. 8. Heat release profiles at  $\sigma = 100 \text{ g/m}^3$

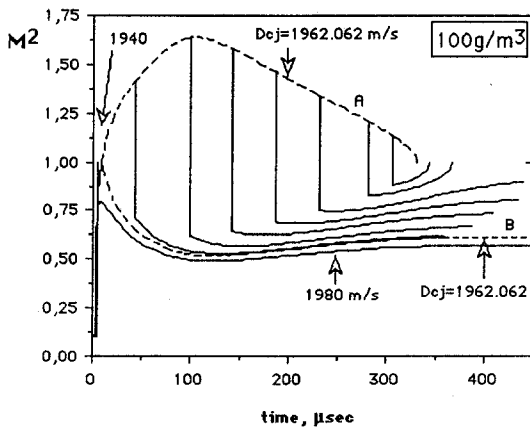


Fig. 7. Integral paths of Mach number (squared) at  $\sigma = 100 \text{ g/m}^3$

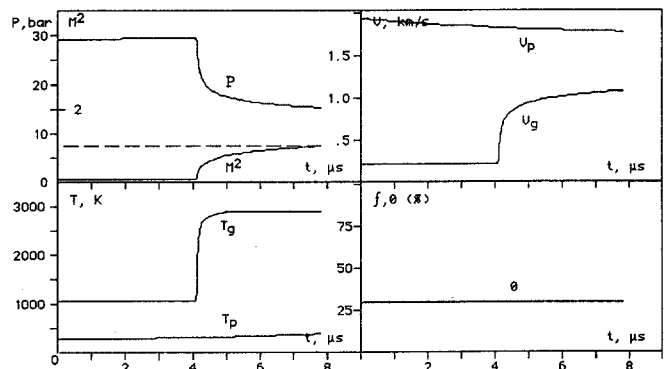


Fig. 9. Structure of pseudo-gas detonation (PGD) at  $\sigma = 200 \text{ g/m}^3$

front. The results of such attempts are shown in Figs. 6–8 and demonstrate that truly steady DFD may exist and be stable (in the sense of the classical theory of detonation (Zel'dovich and Kompaneets 1960): integral curves behind the secondary shock result either in choking for  $\tau < \tau_{CJ}$  or in overdriven solution for  $\tau > \tau_{CJ}$ ). In the case of Fig. 6, the time delay  $\tau$  between the two fronts of steady DFD is between 230 and 280  $\mu\text{s}$  (exactly  $\tau = 241 \mu\text{s}$ ). Mach number for this DFD solution becomes greater than unity in the rarefaction wave after passage through the second CJ point, which is located at  $\tau = 400 \mu\text{s}$ .

It is interesting to note that the secondary shock wave affects the two-phase flow in very important manner so that one can see even three maxima of energy release (Fig. 8) instead of only two, like in Fig. 2 (note that at the second CJ point  $dq_+/dt = dq_-/dt$ , i.e. energy release has a maximum). This is due to rapid re-intensification of velocity and temperature relaxation processes behind the front of the second discontinuity. This feature will be discussed in the next section where the structure of DFD is displayed in details.

## 6. Detonation structures

Typical full structures of the above mentioned different detonation regimes are shown for comparison in Figs. 9–12: pseudo-gas detonation PGD (Fig. 9) at particle concentration  $\sigma = 200 \text{ g/m}^3$ , single-front detonation SFD at  $\sigma = 200 \text{ g/m}^3$  (Fig. 10) and  $1200 \text{ g/m}^3$  (Fig. 11), and double-front detonation DFD at  $\sigma = 500 \text{ g/m}^3$  (Fig. 12). The left upper parts of those figures show the profiles of pressure and local Mach number (squared) in a frame fixed to the detonation front. The left bottom parts of those figures illustrate the behavior of temperatures of gas ( $T_g$ , upper curves) and particles ( $T_p$ ). The right upper parts show the velocities of particles  $v_p$  and gas  $v_g$  (the velocity of particles at the front equals to  $D_{CJ}$ ). The right bottom parts of the figures display the profiles of volume fraction of oxidizing gaseous components ( $\phi$ ) reacting with aluminum, and mass fraction of burnt aluminum  $f$  ( $f$  equals to zero prior to the ignition of particles). Results correspond to the same mixture as above, for which the ideal CJ detonation velocity in the pure gas mixture ( $\sigma = 0$ ) equals to 1999 m/s.

In the PGD wave ( $\sigma = 200 \text{ g/m}^3$ ,  $D_{CJ} = 1938 \text{ m/s}$ , see Fig. 9), aluminum particles are heated and accelerated by the gas flow only slightly. In the gas induction zone up to  $t = 4 \mu\text{s}$ , pressure, temperature and velocity of gas remain



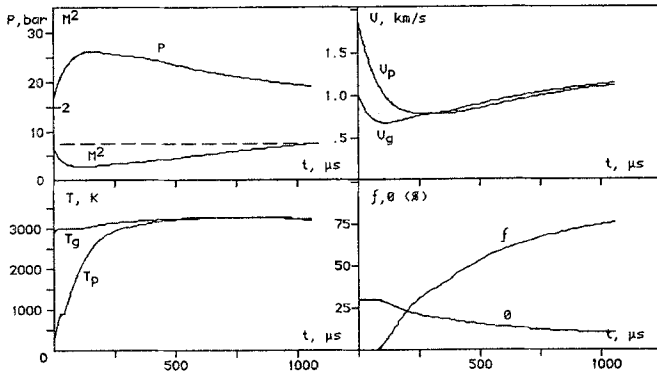


Fig. 10. Structure of SFD at  $\sigma = 200 \text{ g/m}^3$

practically unchanged, but after the beginning of exothermic gas reactions, sharp decrease of pressure along with increase of gas temperature and velocity is seen. The CJ plane is located at  $t = 8 \mu\text{s}$ . The particles are not ignited inside the steady zone and equilibrium of velocity as well as of temperature between particles and gases is not reached at the end of this zone. So, this solution does not differ (in the steady zone) from the case of "inert" particles suspended in the same gaseous mixture (that is, the same particles having all physical characteristics identical, but non-reactive).

Fig. 10 shows the structure of hybrid SFD at the same particle concentration as in Fig. 9, i.e. at  $\sigma = 200 \text{ g/m}^3$ . The value of detonation velocity is now  $D_{CJ} = 1954 \text{ m/s}$ . One can see the melting of particles at  $T_p = T_m = 933 \text{ K}$ ; ignition of particles occurs later, when their temperature reaches  $1350 \text{ K}$ . The CJ plane is located here at  $t = 1050 \mu\text{s}$  ( $X_C = 0.9 \text{ m}$ ). In Fig. 10, the resolution at the vicinity of the shock front is not sufficient to see the initial part of the profiles, but in this case, they are similar to those for pseudo-gas detonation shown on Fig. 9. Only 75% of aluminum is burnt inside the steady reaction zone, then the energy loss rate overtakes the energy release rate. At the CJ plane, gas and particle temperatures and velocities are very close one another, i.e. products of nonideal detonation are practically in equilibrium. Note that velocity relaxation in the considered case is faster than the temperature relaxation. Thus, in the hybrid mixtures under study, at the same particle concentration (e.g.  $\sigma = 200 \text{ g/m}^3$ ) two different regimes of nonideal detonations may propagate – PGD and SFD. This is an example of the possibility for multiple propagation regimes to exist in this kind of mixtures. This point will be discussed later in Sect. 8.

Another example of SFD structure is shown in Fig. 11, but at  $\sigma = 1200 \text{ g/m}^3$ . In this case,  $D_{CJ} = 1358 \text{ m/s}$  and the CJ plane is located at  $t = 3000 \mu\text{s}$  ( $X_{CJ} = 1.9 \text{ m}$ ). Due to the lower detonation velocity and the larger particle concentration, the duration of the induction zone for the gas reactions becomes here much larger, so that a first pressure maximum is discernible in Fig. 11 (whereas it was not possible to observe in Fig. 10, due to the resolution of the plotting): this first part of the pressure evolution is similar to that observed for PGD (Fig. 9). Aluminum burnt fraction in this case is only about 20%, due to insufficient amount of gaseous oxidizing components. Because the reaction zone

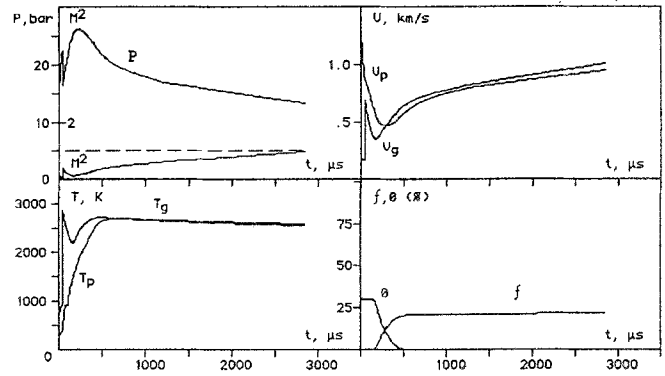


Fig. 11. Structure of SFD at  $\sigma = 1200 \text{ g/m}^3$

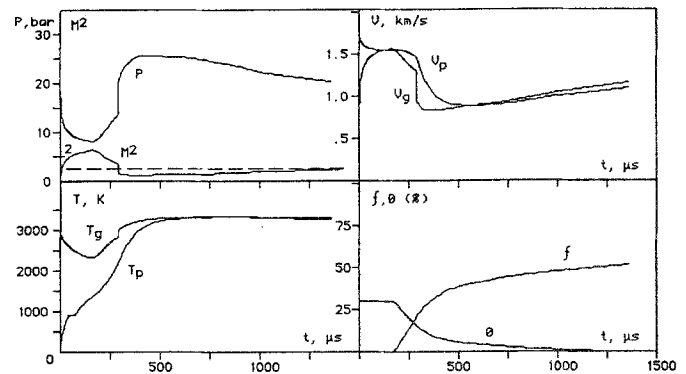


Fig. 12. Structure of DFD at  $\sigma = 500 \text{ g/m}^3$

length of the steady SFD at  $\sigma = 1200 \text{ g/m}^3$  is essentially greater than at  $\sigma = 200 \text{ g/m}^3$ , it is possible to conclude that the detonability of the rich hybrid mixtures with relatively high aluminum particle concentrations is lower than that of lean hybrid mixtures – at least the travel distance to reach steady detonation should be essentially larger in the case of rich mixtures. This also emphasizes the necessity of investigating the effect of particle size and shock tube diameter on the reaction zone length of hybrid detonation.

The double-front detonation (DFD) structure is illustrated in Fig. 12 for particle concentration  $\sigma = 500 \text{ g/m}^3$ . One can see that the secondary shock front takes place significantly before the interphase equilibrium be reached, and that this shock reintensifies the interphase exchanges. At this particle concentration, SFD does not exist, but PGD exists: note that the structure of the leading part of DFD up to the first CJ point is identical to the structure of the PGD wave corresponding to  $\sigma = 500 \text{ g/m}^3$ .

Thus, the examples shown above demonstrate that there exist very important differences between the structures of PGD, SFD and DFD and that one can shift from one structure to another one following the particle concentration. Experimental evidence of the existence of propagation regimes exhibiting such structures has already been displayed in different hybrid two-phase mixtures (see Veysière 1986). In Fig. 13 are shown pressure records of PGD and DFD in a hydrogen-air-aluminum particles mixture, and in Fig. 14 pressure records of SFD in a hydrocarbon-air-aluminum

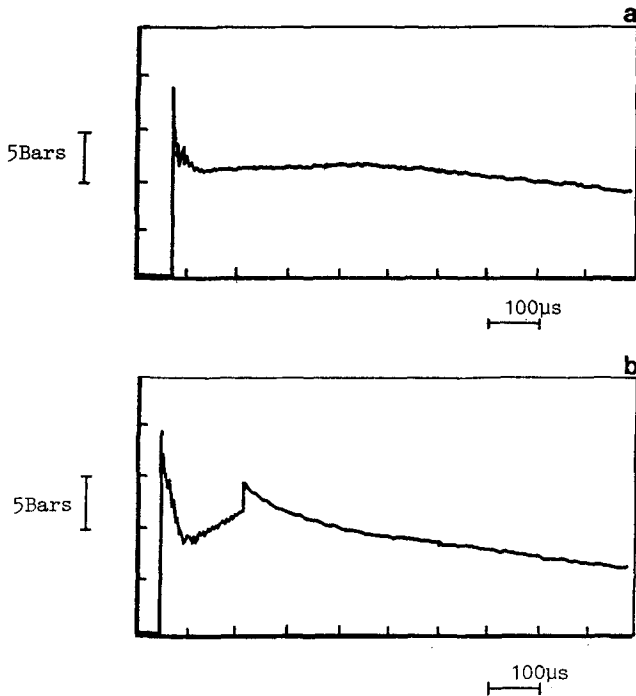


Fig. 13. Examples of experimental pressure profiles recorded in a hydrogen/air mixture ( $r = 1.06$ ) with  $13 \mu\text{m}$  aluminum particles. **a** PGD ( $\sigma = 20 \text{ g/m}^3$ ); **b** DFD ( $\sigma = 65 \text{ g/m}^3$ )

particles mixture. However, the amount of available experimental results is still restricted to the range of low concentrations of particles ( $\sigma < 300 \text{ g/m}^3$ ), since at higher concentrations it is difficult to perform experiments in well controlled initial conditions (non uniformity of dust dispersion). Therefore, another interest of the present modelling is to allow easily a parametric investigation of the non-ideal detonation waves in hybrid two-phase mixtures. In the next paragraph, we examine the dependence of the structure of non-ideal detonations on the fundamental parameters of the hybrid mixture.

## 7. Dependence of the structure on the fundamental parameters of the system

As we pointed out in Sect. 2, the structure of non ideal detonation in a hybrid mixture is extremely dependent on the particular form of the energy evolution, as the existence of steady solutions is determined by the possibility to achieve or not the sonic condition at the points of the flow where  $dq/dt = 0$ . The rate of effective energy release is determined by the competition between different sources of energy release and energy loss in the flow. To get a more precise idea of the conditions in which the above displayed different regimes and corresponding structures may be achieved, we have studied the combined influence of the concentration of aluminum particles with their size, the losses to the walls, and the gaseous composition. The influence of these different parameters has been examined in more details in previous papers (Khasainov and Veyssi re 1991b, 1993). Here, we shall summarize only the main results of these works.



Fig. 14. Example of experimental pressure profile of SFD recorded in an ethylene/air mixture ( $r = 1.15$ ) with  $13 \mu\text{m}$  aluminum particles ( $\sigma = 60 \text{ g/m}^3$ )

### Effect of particle size

In Fig. 15 are plotted the values of the detonation velocity as function of the particle concentration for different values of the particle diameter, in the same gaseous mixture as above (hydrogen-air with equivalent ratio 1.06). For a particle diameter  $dp = 20 \mu\text{m}$  (Fig. 15a), when the particle concentration  $\sigma$  increases from 0, steady PGD solution exists and its velocity decreases with increasing  $\sigma$ . As discussed in Sect. 6, this evolution corresponds to a "dilution" of the mixture by "inert" particles. At a given concentration  $\sigma_{qi}$  (here  $\sigma_{qi} = 1200 \text{ g/m}^3$ ), the detonation velocity rapidly drops, indicating that the quenching limit by inert particles has been reached. However in the case of reactive particles, beyond this limit hybrid steady SFD exists having a low velocity of propagation. This situation corresponds to a large unique reaction zone, due to the long time delay for aluminum particles to ignite behind the leading shock wave.

When the diameter of particle decreases, the concentration corresponding to quenching limit by "inert" particles ( $\sigma_{qi}$ ) diminishes. Moreover, before reaching this limit, DFD and SFD may be obtained in certain domains of particle concentration. Let us recall that the detonation velocities of PGD and DFD solutions are identical, but they totally differ by their structure behind the leading front. Dependence of the DFD structure on the diameter of particles is displayed in Fig. 16, where are plotted the values of the delay  $\tau$  between the two fronts of DFD as function of particle concentration, for different particle diameters in the range  $10\text{--}18 \mu\text{m}$ . From the results of Figs. 15 and 16, one can establish that the DFD structure exists only for a suitable choice of concentration and size of the solid particles. The range of particle diameters able to give rise to this structure is quite narrow. The variation of the domain of existence of DFD as function of the particle diameter may be explained qualitatively on the basis of the balance between  $dq_+/dt$  and  $dq_-/dt$  (Eq. 31), according to the value of  $dq_+/dt \approx \sigma_{po} Q_{Al} \phi^{0.9} / d_{po}^2$  provided by Eq. 30: indeed, for the left branch of DFD domain, an increase of the particle diameter can be compensated by an increase of the particle concentration  $\sigma$ ; for the right branch of DFD domain, the opposite dependence is observed since this branch corresponds to "rich" mixtures (as regarding aluminum proportion) and in this case, addition of aluminum particles decreases the specific heat release. In Fig. 16, we have plotted also the values of the delay  $\tau$  between the

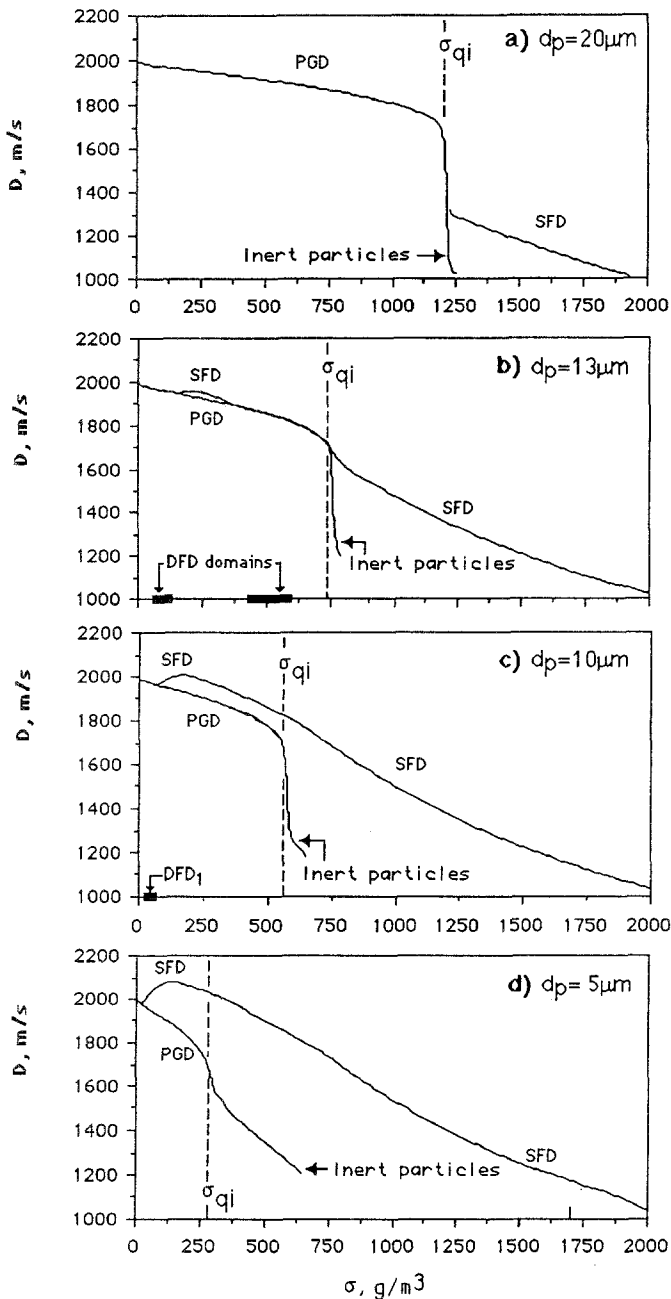


Fig. 15a-d. Dependence of the detonation velocity on the mass particle concentration for decreasing values of the particle diameters

two fronts measured in the experiments performed in the same mixture with  $13 \mu\text{m}$  aluminum particles (see Veyssi re 1986): the experimental values match satisfactorily the numerical values of the “left” branch of the DFD domain. Unfortunately, no experimental results are available for the “right” branch, on account of the great technical difficulties to perform experiments in well controlled conditions (uniformity of particle distribution inside the detonation tube) at high particle concentrations ( $> 300 \text{ g/m}^3$ ).

Moreover, when the diameter of particles becomes too large ( $> 19 \mu\text{m}$ ), DFD is replaced by PGD (according to equation (30), the energy release rate diminishes, thus the energy loss rate promoted by the particles and the walls

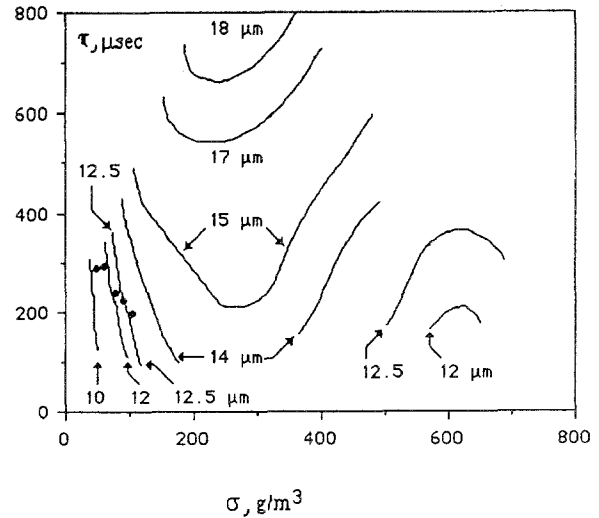


Fig. 16. Dependence of the delay  $\tau$  between the two fronts of DFD on particle concentration and diameter: — calculated values, • experimental values measured with  $13 \mu\text{m}$  aluminum particles

becomes predominant). On the opposite, when the diameter of particles diminishes under a critical value ( $9 \mu\text{m}$ ), DFD is replaced by SFD (in this case, equation (30) indicates that the energy release rate due to particle burning increases; hence, it becomes greater than energy losses). In Fig. 15, one also can note that, for the smallest particles, the heat release due to burning of particles may occur sufficiently soon to allow a significant increase of the detonation velocity, beyond the value of the detonation velocity of the gaseous mixture without particles.

The preceding results emphasize the ambivalent role played by solid particles, which on one hand, at first pull out part of the energy released by gaseous reactions to heat up and accelerate, and, on the other hand, bring after some delay additional heat to the mixture by their combustion. Thus, when increasing the concentration of particles of a given size, the two effects are modified, but the processes do not occur in the same characteristic times, hence the complexity of predicting the propagation regime which will be obtained.

#### Effect of heat losses

Investigation of the effect of tube diameter provides a manifest illustration of the role played by the losses inside the reaction zone on the structure of non-ideal detonations. In all results shown above, the diameter of the detonation tube is assumed to be 69 mm, which corresponds to the diameter of the tube used by Veyssi re (1986) for his experiments. Here, we have varied the diameter of the confinement by ascribing an arbitrary multiplying coefficient to the nominal diameter of the tube (this is a ratio, the numerator of which is changed; thus, the value 15/15 for this factor corresponds to the nominal tube diameter used above, and 30/15 to a 138 mm tube diameter). As can be seen in Fig. 17, the range of tube diameters for which steady DFD structure exists is rather narrow and may be analyzed in the same way as above for the effect of particle diameter. Results of Figs. 17 and 18 indicate that DFD is replaced by SFD, when the tube

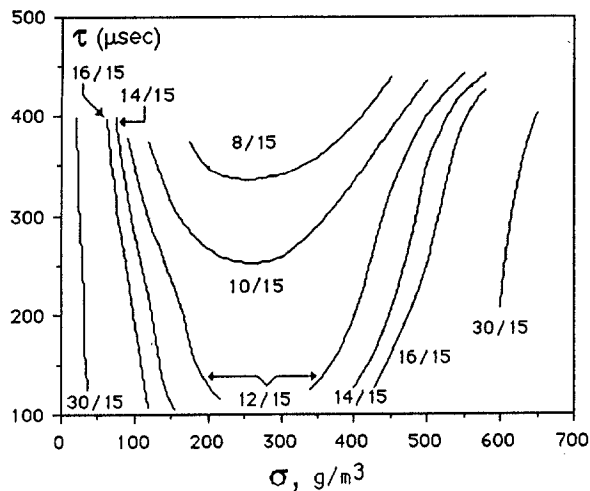


Fig. 17. Influence of the shock tube diameter on the variation of the delay  $\tau$  between the two fronts of DFD with particle concentration

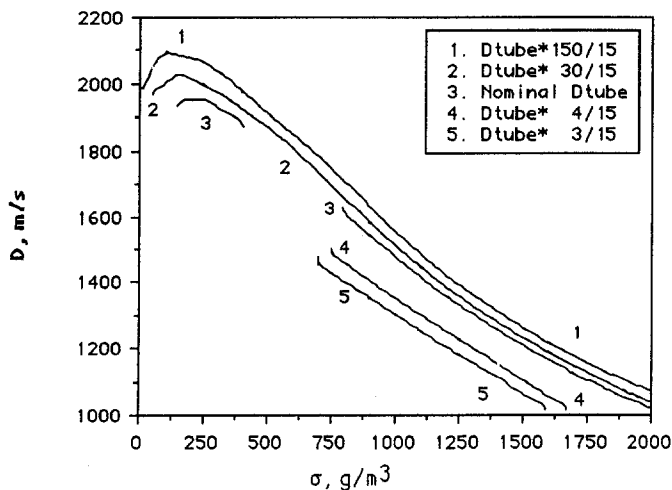


Fig. 18. Influence of the shock tube diameter on the domain of existence of SFD

diameter increases (in this case, the energy loss rate diminishes). On the opposite, for smaller tube diameters, DFD is replaced by PGD (because the energy loss rate overtakes the energy release rate). Therefore, we reach qualitatively the same conclusions as for the effect of particle size, on the fundamental mechanisms governing the detonation structure of non-ideal detonations; but here we have varied only the energy loss rate, without modifying the rate of heat release from chemical reactions.

There is another source of energy losses of practical interest, which is a polydisperse distribution of solid particles. Indeed, in practical situations all the particles have not the same diameter and there exists a scattering of particle size with the possibility for very fine and very large particles to coexist in the mixture, corresponding to the boundaries of the size distribution domain. Calculations performed with a bimodal distribution of particles (with a fraction of the total mass of particles having the nominal  $13 \mu\text{m}$  diameter and the remaining a diameter 10 or 20 times larger) have shown

(Khasainov and Veyssi re 1993) that, in this case, the domains of existence of steady propagation regimes are shifted to higher particles concentrations, due to the decrease of the effective concentration of "fine" particles in the total mass and the increase of energy losses introduced by the presence of coarse particles (which is again consistent with Eq. 30). Even, we have demonstrated that with a proper choice of the relative mass fractions of fine and coarse particles, it is possible to replace the effect of the tube walls by the effect of coarse particles and get truly steady non-ideal detonations in unconfined conditions. In this case, the coarse particles behave as an energy sink and provide a sufficient amount of energy losses to allow that the effective energy release rate  $dq_{\text{eff}}/dt$  becomes equal to zero in some part of the flow.

#### Effect of gaseous composition

The role of gaseous composition is not easy to predict as there exists a competition between gaseous reactants and solid particles to combine with the gaseous oxidizing components. To study this effect, we have considered different hydrogen-air mixtures, the equivalence ratio of which has been varied from lean ( $r \approx 0.6$ ) mixtures to very rich ( $r > 3.0$ ) ones. It is worthy to recall that in the case of aluminum, the particles may react not only with  $\text{O}_2$ , but also with  $\text{H}_2\text{O}$ ,  $\text{CO}_2$  and even  $\text{H}_2$ . Thus, the possibility of burning of solid particles in the products of gaseous reactions is insured in any conditions. Examples of dependence of the detonation velocity on the concentration of aluminum particles are shown in Fig. 19 for  $r = 0.78$  and in Fig. 20 for  $r = 1.5$ . These figures display many similarities with Figs. 15d and 15b respectively. In Fig. 19, we have plotted the experimental results obtained by Veyssi re (1985) for particle concentrations in the range of  $0\text{--}150 \text{ g/m}^3$ . These results strongly suggest the existence of an abrupt change in the evolution of detonation velocity in the vicinity of  $\sigma = 50 \text{ g/m}^3$ , which is in very good agreement with the predictions of the theoretical model. Moreover, it can be shown that, for very rich mixtures ( $r > 3$ ), SFD exists at large particle concentrations, whereas PGD becomes the predominant propagation regime for moderate values of  $\sigma$  (case similar to that of Fig. 15a). Yet, there exists an intermediate domain of gaseous composition where steady DFD may exist. In this case, the numerical results are in reasonable agreement with the available experimental results (see Veyssi re and Khasainov 1991a). Further details about the influence of gaseous composition may be found elsewhere (Veyssi re and Khasainov 1991a,b). Qualitatively, one can conclude by analogy that the energy release rate is decreased when changing from lean to rich mixtures, that is, addition of heat by burning of solid particles is easier in lean mixtures, which favour the formation of SFD. On the opposite, in very rich mixtures the heat release from solid particles does not occur sufficiently rapidly for allowing SFD to be formed (however, Eq. 30 shows that decrease of  $Q_{\text{Al}}$  could be compensated by decrease of particle size).

All the above examples indicate the complex dependence which exists between the fundamental physical parameters of the system and the actual process of energy release which determines the existence of the different steady solutions. The change of only one parameter of the system induces, in general, marked modifications of both processes of energy

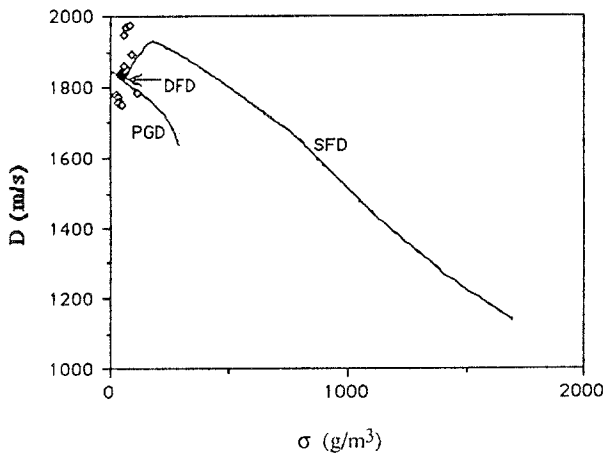


Fig. 19. Dependence of the detonation velocity on the mass particle concentration for a lean gaseous mixture ( $r = 0.78$ ). — calculations;  $\diamond$  experimental values

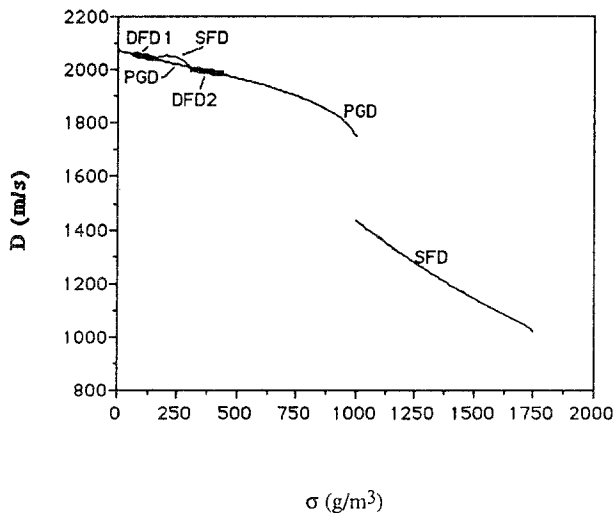


Fig. 20. Dependence of the detonation velocity on the mass particle concentration for a rich gaseous mixture ( $r = 1.5$ )

release and energy losses. The situation is even more complicated, due to the possibility for multiple solutions to exist for a fixed set of the parameters of the system. We examine this problem in the next section.

## 8. The problem of multiplicity of solutions

### *The Kuznetsov theory*

In the examples shown in the previous sections, we have displayed several times that more than one steady propagation regime of non-ideal detonations could exist for the same choice of parameters of the mixture (see for example Sects. 5 and 6). It is worthy to recall that the theory of non-ideal detonations derived from the ZND model is built by taking into account mechanical and heat losses in the reaction zone. Generalizing this model to the case of nonmonotonic energy release in homogeneous mixtures, Kuznetsov (1967 and

1968) has shown that detonation mode could be nonunique, according to the actual energy release process. According to Kuznetsov's results, in the case of an arbitrary nonmonotonic energy release, the generalized theory of nonideal detonations predicts that the total number of possible detonation regimes is odd. If the detonation mode is unique, it is stable. If there exist several detonation modes, those with odd order are stable (these regimes correspond to local maxima of energy release) and the intermediate even ones are unstable (in the Kuznetsov analysis, modes are considered stable or unstable against transformation into one another under infinitely small perturbations). As a result, detonation waves propagating at the highest and lowest velocities are stable. Namely, in the case of one maximum of energy release downstream of the shock front this theory predicts the existence of stable "normal" and "low" velocity detonations along with intermediate unstable detonation regime. But in some ranges of governing parameters, only either normal or low velocity detonation regime may propagate. It is not out of interest to note that the first example of nonmonotonic energy release to which Kuznetsov applies his theory, is the case for which transition to the equilibrium state behind the shock wave occurs through the competition between a heat release mechanism and heat absorption one, which is a situation often met when solid particles are suspended in a gaseous detonable medium. Here, we shall examine this problem in the case of heterogeneous hybrid mixtures, e.g. gaseous reactive mixtures with suspended combustible solid particles.

### *Multiplicity of solutions in hybrid mixtures*

Because the energy release in the hybrid two-phase mixtures is generally nonmonotonic, then the possibility arises of multiple solutions for a given gaseous composition of the mixture with a certain mass concentration of particles of given diameter. The precise profile of the energy evolution curve will depend on the particular values of the governing parameters. But, on account that the characteristic reaction rates for gases and particles may differ by an order of magnitude (or even more), the energy release from the mixture components takes place in two steps and there may be two maxima in the energy release profile behind the shock front. According to Kuznetsov (1968), the number of solutions in this case may vary from one to five. Let us examine the results of our investigations in the case of the hydrogen-air mixture (equivalent ratio  $r = 1.06$ ) with a suspension of  $13 \mu\text{m}$  aluminum particles which has been studied in the previous sections. In Fig. 21, the dependence of the detonation velocity on particle mass concentration is plotted. This figure summarizes the regions of existence of PGD, SFD and DFD in the mixture under study:

1) The first family of detonation solutions (branches  $\text{PGD}_1$ ,  $\text{PGD}_2$  and  $\text{PGD}_{3i}$ ) which corresponds to the first appearance of  $dq_{\text{eff}}/dt = 0$  (with  $d^2q/dt^2 < 0$ ), represents the pseudo-gas detonation. The dependence of detonation velocity  $D$  on particle concentration  $\sigma$  computed for the branches  $\text{PGD}_1$  and  $\text{PGD}_2$  shown in Fig. 21, corresponds to the non-ignition of aluminum particles upstream of the CJ point and exactly coincides with the results obtained in considering the case of "inert" aluminum particles. The

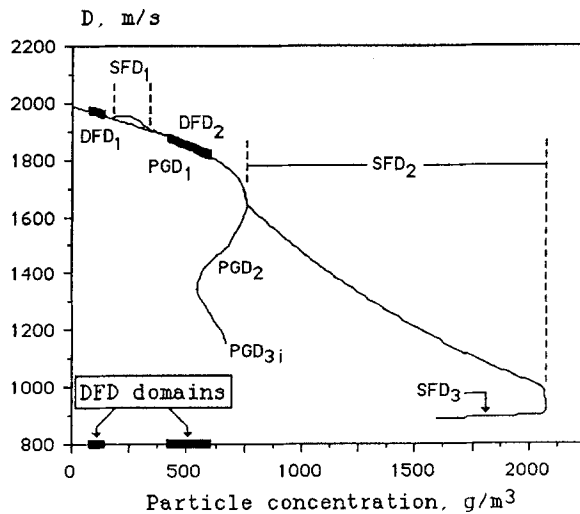


Fig. 21. Velocities of PGD, SFD and DFD as function of particle concentration for the mixture  $r = 1.06$ . Existence of multiple solutions

low-velocity detonation branch  $PGD_{3i}$  exists only for the case of inert particles (see below).

The decrease of  $D_{CJ}$  when particle concentration augments along “normal” and “low” detonation velocity branches  $PGD_1$  and  $PGD_{3i}$  is due to the increase of losses related to the heating and acceleration of the particles in the wave. From the mathematical point of view the pseudo-gas detonation solution corresponds to  $M = 1$  and first maximum of effective energy release downstream of the shock front. Branches  $PGD_1$  and  $PGD_{3i}$  are stable, but intermediate branch  $PGD_2$  is unstable (Zel’dovich and Kompaneets 1960). Thus, the pseudo-gas solution is well in accordance with the general theory of nonideal detonations with non-monotonic energy release (Kuznetsov 1967, 1968). This part of our results matches also the predictions of Menga (1981) who treated the influence of inert particles on the detonation of a gaseous mixture.

2) The second family of detonation solutions corresponds to SFD waves, i.e. when aluminum burning contributes to the overall energy release ( $SFD_1$ ,  $SFD_2$  and  $SFD_3$  branches in Fig. 21): this situation is met at the second appearance of  $dq_{eff}/dt = 0$  with  $d^2q/dt^2 < 0$ . In the mixture considered, we have found only two main regimes of SFD: normal velocity solution which consists of two separate stable branches  $SFD_1$  and  $SFD_2$ , and unstable branch  $SFD_3$  with  $D = 800-900$  m/s (this last case corresponds to very high ignition delays of particles – several tens of millisecond). The attempts to find another stable LVD branch with  $D < 800$  m/s were unsuccessful due to extremely large gas induction times. The existence of only one stable solution for SFD family (consisting of  $SFD_1$  and  $SFD_2$  branches) is probably related to the influence of the ignition temperature of particles  $T_{ign}$ : it is evident that particles cannot be ignited behind a shock of given strength if the shock amplitude is too low (see for example Borisov et al. (1991)) or if  $T_{ign}$  is too high. In this case SFD regime cannot propagate.

3) At the present state of our investigations, we have been unable to find numerically other solutions. By the way, it is worthy to note that we have rejected from the set

of authentic solutions, one particular situation not easy to analyze: for this case (met for  $\sigma > 550$  g/m<sup>3</sup> and velocity of the leading front in the range 1100–1400 m/s), there was a formal convergence toward a detonation velocity value by try and error technique, but careful examination of the families of integral paths surrounding this value revealed that there existed an important distance between the positions of the points corresponding to the conditions  $dq_{eff}/dt = 0$  and  $M = 1$  in two integral paths of opposite nature. This discrepancy cannot be overcome by increasing the accuracy, so the existence of a saddle point type solution may not be expected in this case. This situation is an “*a posteriori*” illustration of the necessity to treat carefully the equivalent CJ condition in the reaction zone of non-ideal detonations (Zel’dovich et al. 1988). This kind of difficulty was met near critical conditions of particles ignition at relatively low detonation velocities. However, changing arbitrarily the value of the ignition temperature of solid particles did not permit to escape this situation; so, it seems possible to dismiss a reason of numerical nature for being responsible of this behavior.

#### Discussion

In the case of hybrid mixtures, there are, in general, two local maxima of energy release  $q$  and, according to the theory of nonideal detonations (Kuznetsov 1967, 1968) in certain particle concentration ranges it is possible to expect up to 5 different solutions – 3 of them should be stable and 2 unstable. Here, the following cases are met with increasing concentration of particles (see Fig. 21):

- for  $\sigma < 165$  g/m<sup>3</sup>, only the pseudo-gas ( $PGD_1$ ) solution exists. There is no SFD at all, because particles fail to ignite upstream of the CJ plane, and in this concentration range only pseudo-gas detonation  $PGD_1$  may propagate.

- for  $165$  g/m<sup>3</sup>  $< \sigma < 375$  g/m<sup>3</sup>, two solutions exist: PGD and SFD. From the mathematical point of view, SFD solution corresponds to  $M = 1$  and second maximum of energy release ( $dq_{eff}/dt = 0$  with  $d^2q/dt^2 < 0$  downstream of the shock front, whereas the PGD solution corresponds to the first maximum of  $q$ . These two solutions ( $PGD_1$  and  $SFD_1$  branches) are stable in the sense of the above mentioned definition. According to the theoretical predictions of Kuznetsov (1967), a third unstable solution should exist between PGD and SFD. However, we have been unsuccessful in displaying numerically any intermediate solution between the  $PGD_1$  and  $SFD_1$  branches. This fact seems to contradict to the theory (Kuznetsov 1967, 1968). Such a discrepancy in the number of solutions with theoretical predictions has also been displayed by Voronin and Zhdan (1984), however in a situation somewhat different of the present one (detonation of cryogenic hydrogen-oxygen mixtures).

- for  $375$  g/m<sup>3</sup>  $< \sigma < 550$  g/m<sup>3</sup>, only the pseudo-gas solution exists again. In this range of particle concentration, when increasing  $\sigma$ , the exchanges between gases and particles to heat up and accelerate the particles, are such that the rate of energy losses increases more rapidly, so that particles are not ignited upstream of the CJ plane and SFD cannot exist.

– for  $550 \text{ g/m}^3 < \sigma < 750 \text{ g/m}^3$ , three solutions are found, corresponding to the three PGD<sub>1</sub>, PGD<sub>2</sub>, PGD<sub>3i</sub> branches described above.

– for  $750 \text{ g/m}^3 < \sigma < 1600 \text{ g/m}^3$ , a unique solution is found consisting of the stable SFD<sub>2</sub> branch.

– for  $1600 \text{ g/m}^3 < \sigma < 2080 \text{ g/m}^3$ , two SFD solutions exist, the stable branch SFD<sub>2</sub> (continuation of the preceding one), where detonation velocity decreases from 1650 m/s to 950 m/s, and the unstable one SFD<sub>3</sub>. Solutions with lower detonation velocity do not exist due to the restrictions caused by ignition criteria of particles and gas. It is probably the reason why a stable branch with even lower detonation velocity values (that is, an additional odd solution) has not been found.

A particular treatment must be reserved to the case of double-front detonations (DFD). This particular regime is characterized by the existence of two discontinuity fronts, the first one being supported by the energy release from gaseous reactions and the second one by the energy release coming from the burning of solid particles in hot ambient products. As mentioned above, the first detonation wave of DFD corresponds exactly to the PGD solution calculated at the same particle concentration: detonation velocity is the same, parameter profiles are identical. The difference between PGD and DFD solutions lies in the fact that in the case of PGD, beyond the CJ point the steady region is followed by an unsteady flow, whereas in the case of DFD, the first steady region is bounded beyond the CJ point by a second steady region adjacent to it and having the same velocity; this second region is followed by the unsteady flow, downstream of the second CJ point. That is to say that the existence of this secondary detonation zone has no influence on the leading wave. Thus, as regarding the problem of selection of suitable detonation velocities which are solutions of the system of ordinary differential equations, there are no difference between PGD and DFD. As a result, it does not seem to us that they can be counted as separate solutions within the frame of the theory of non-ideal detonations with nonmonotonic energy release. On the opposite, according to the flow parameter profiles downstream of the first CJ point, DFD must be regarded as a distinct regime. This has been evidently shown experimentally (Veyssi re 1986) and numerically (Khasainov and Veyssi re 1991a). From the practical point of view, it is of great importance to know the conditions for which DFD can exist, especially the particle concentration range. In the studied mixture, as indicated in Fig. 21, DFD exists for  $80 \text{ g/m}^3 < \sigma < 165 \text{ g/m}^3$  (DFD<sub>1</sub> branch) and for  $400 \text{ g/m}^3 < \sigma < 600 \text{ g/m}^3$  (DFD<sub>2</sub> branch), that is, in particle concentration domains where PGD exists but SFD cannot exist. As demonstrated previously (Khasainov and Veyssi re 1991b), along the DFD<sub>1</sub> branch the delay between the two detonation fronts diminishes with increasing particle concentration, and, on the opposite, augments with particle concentration along the DFD<sub>2</sub> branch (see Figs. 16, 17). Dependence of DFD on the fundamental parameters of the system has been described above in Sect. 7.

Following the above results, the occurrence of multiple detonation modes due to nonmonotonic energy release can be regarded as possible for heterogeneous hybrid mixtures. However, certain inconsistencies with the theoretical

predictions remain not well elucidated: the problem of non-existence of an unstable steady solution between the PGD<sub>1</sub> and SFD<sub>1</sub> branches has been already observed numerically in a close situation by Voronin (1984) for cryogenic hydrogen-oxygen mixtures. As for the fact that the maximum number of solutions found here is three instead of five, the most likely explanation lies in the restrictions caused by ignition criteria of particles and gases. In other respects, the theoretical model of Kuznetsov does not predict the existence of DFD propagation regimes.

Another problem is to get the experimental evidence of these multiple regimes, and especially of low-velocity detonations (LVD). Though the number of available examples is, up to now, quite limited, some of them have been provided by the study of detonation of gaseous mixtures in inert heterogeneous media: Saint-Cloud (1976) observed low-velocity detonation regimes in mixtures of combustible gases with water foams, and Mamontov et al. (1980) displayed such regimes with acetylene-oxygen mixtures in shock tubes filled with inert particles of sand or steel. But, to our knowledge, experimental confirmation has not been got in hybrid mixtures yet now. The reason lies in the difficulty of performing experiments in well controlled initial conditions at high particle concentrations.

Further conclusions may be derived from the results of the approximate analysis of Khasainov et al. (1979). In particle concentration ranges where only PGD exists, secondary compression waves (i.e. waves without gasdynamic discontinuity) may be generated with time behind the CJ point of the PGD wave due to ignition and burning of particles; however, these secondary waves have no sufficient strength to form a supersonic flow behind the PGD sonic plane and to overtake the leading PGD wave (see also Khasainov and Veyssi re 1988). In the case when both PGD and SFD exists, by analogy with the results of Khasainov et al. (1979), it is possible to imagine that, with a strong enough initiation source it should be possible to initiate the SFD directly. On the opposite, in the case of a relatively weak initiation source, after a certain delay steady PGD will propagate in the initial part of the shock tube. But, after the ignition of aluminum particles downstream of the CJ plane of the leading pseudo-gas detonation, secondary compression waves would arise since the particle concentration is suitable for a SFD to propagate. The SFD build-up will take place when this secondary compression wave overtakes the leading detonation front. This problem needs a particular study. Indeed, as mentioned above, PGD may be regarded as being stable under *infinitely small* perturbations regardless of the fact that delayed ignition and reactions of aluminum particles can take place far behind the CJ plane of PGD. However, the approximate analysis of Khasainov et al. (1979) indicates qualitatively that PGD could propagate steadily during a finite period of time and, then, the velocity of the leading front should be changed to that of SFD. But, in the frame of the present steady model, it is not possible to analyze the problem of stability of the different detonation regimes under the influence of *finite* perturbations. Investigating this problem requires to use unsteady modelling of non-ideal detonations. Thus, this question will be not treated within the frame of the present paper. In the same way, when both PGD and DFD exist, energy release from reactions of parti-

cles behind the PGD wave result with time in formation of a secondary discontinuity wave which will propagate steadily behind the leading PGD wave as a secondary detonation wave. Complete analysis requires also unsteady modelling.

## 9. Conclusions

From the results shown in the present paper, it is obvious that the prediction of the critical conditions for the existence of a steady propagation regime of a nonideal detonation, as well as the prediction of the characteristic flow parameters of the wave, are a very complicated problem in the case of heterogeneous hybrid mixtures. Analysis of this problem has been performed with the help of an approximate numerical model in the case of a mixture of hydrogen and air with suspended aluminum particles. The existence or not of steady propagation regimes is strongly dependent on the characteristic features of the effective energy release profile. In hybrid mixtures, the effective energy release process is generally nonmonotonic and is governed by the competition between the different processes of energy release provided by the combustion of gaseous and solid components of the mixture, and the different energy losses towards the particles for accelerating and heating up in the gas flow and also towards the walls of the confinement. In the situation studied here, we have displayed three kinds of propagation regimes: Pseudo-Gas Detonation (PGD), Single-Front Detonation (SFD) and Double-Front Detonation (DFD). The critical values of the characteristic parameters (concentration and size of solid particles, gaseous composition, dimensions of the detonation tube) which influence the existence of those different regimes, can be determined with our approximate numerical model and match the experimental results we had got previously. Moreover, we have been able to predict the possibility of multiple detonation regimes for a given composition of the mixture. Further studies would be wishable to study the stability of those solutions and the process of transition to detonation after initiation, but also to get experimental evidence of the multiple regimes, particularly those propagating with a low velocity. However, it seems to us that the validity of some of our results is not restricted by the assumptions made in our model or by the particular characteristics of the medium we have studied, and may be extended qualitatively to situations having similarities with the present one via a nonmonotonic energy release process. The present results show that, with an approximate model taking into account the different characteristic times which govern the processes of energy release by chemical reactions and of energy losses, it is possible to obtain a good global understanding of the phenomenon of propagation of nonideal detonations in complicated situations such as one can meet in the case of two-phase hybrid mixtures. By providing a map of phenomena that can occur, this approach is a necessary step on the way of future full numerical direct simulations of hybrid mixture detonations.

## References

- Borisov AA, Khasainov BA, Veyssi re B, Saneev EL, Khomik SV, Fomin IB (1991) On Detonation of Aluminum Suspensions in Air and Oxygen. *Khimicheskaya Fizika* 10:250–272
- Fan BC, Sichel M (1988) A comprehensive model for the structure of dust detonations. 22nd Symposium (International) on Combustion. The Combustion Institute, Pittsburgh pp. 1741–1750
- Gear CW (1971) Difsob for solution of ordinary differential equations. *Commun. of the ACM* 14:186–193
- Khasainov BA, Ermolaev BS, Borisov AA, Korotkov AI (1979) Effect of Exothermic Reactions Downstream of the CJ Plane on Detonation Stability. *Acta Astronautica* 6:557–568
- Khasainov BA, Veyssi re B (1987) Analysis of the steady double-front detonation structure for a detonable gas laden with aluminium particles. *Archivum Combustionis* 7:333–352
- Khasainov BA, Veyssi re B (1988) Steady, plane, double-front detonations in gaseous detonable mixtures containing a suspension of aluminium particles. *AIAA Progress in Astronautics and Aeronautics* 114:284–299, AIAA, NY
- Khasainov BA, Veyssi re B (1993) Effect of Losses on the Existence of Nonideal Detonations in Hybrid Two-Phase Mixtures. *AIAA Progress in Astronautics and Aeronautics*, AIAA New-York, 153:447–461, AIAA, NY
- Korobeinikov V, Levin VA, Markov VV, Chernyi GG (1972) Propagation of Blast Waves in a Combustible Gas. *Astronautica Acta* 17: 529–537
- Kuznetsov NM (1967) Nonuniqueness and stability of detonation modes. *Soviet Physics JETP* 25: 199–204
- Kuznetsov NM (1968) Indeterminacy and stability of the detonation mode in a bounded medium. *Zh.P.M.T.F.* 9:45–55
- Mamontov GM, Mitrofanov VV, Subbotin VA (1980) Regimes of Gaseous Detonations in Rigid Porous Medium. Detonation. *Chemical Physics of Combustion and Explosion Processes*. Chernogolovka. pp.106–110 (in Russian)
- Menga H (1981) Contribution   l'Etude de l'Influence des Pertes Thermom caniques sur la D tonation dans les m langes h t rog nes. Th se de Docteur Ing nieur, ENSMA, Poitiers, France
- Mitrofanov VV, (1988) Detonation Waves in Heterogeneous Media, Novosibirsk
- Nettleton MA (1987) Gaseous Detonations: their nature, effects and control. Chapman and Hall, London, New York
- Nigmatulin RI (1987) Dynamics of multiphase media Ed. Nauka, Moscow
- Price EW (1984) Combustion of metalized propellants. In: *Fundamentals of solid propellant combustion*. K.K.Kuo, M.M. Summerfield (eds.) *Progress in Astronautics and Aeronautics* 90:479–513, AIAA, NY
- Saint-Cloud JP, Guerraud C, Moreau M, Manson N (1976) Experiments on the propagation of detonations in two-phase mixtures. *Acta Astronautica* 3:781
- Veyssi re B, Manson N (1982) Sur l'Existence d'un Second Front de D tonation des M langes Biphases Hydrog ne-Oxyg ne-Azote-Particules d'Aluminium. *Comptes rendus Acad. Sci.* 295:335–338
- Veyssi re B (1985) Contribution   l' tude de la structure des d tonations dans les m langes gazeux explosifs contenant une suspension de particules solides r actives. Th se de Doctorat et Sciences Physiques, Universit  de Poitiers (France)
- Veyssi re B (1986) Structure of the Detonations in Gaseous Mixtures Containing Aluminium Particles in Suspension. *Dynamics of Explosions*, AIAA Progress in Astronautics and Aeronautics, AIAA, NY 106:522–544
- Veyssi re B, Khasainov BA (1991a) A Model for Steady, Plane, Double-Front Detonations (DFD) in Gaseous Explosive Mixtures with Aluminium Particles in Suspension. *Combustion and Flame* 85:241–253
- Veyssi re B, Khasainov BA (1991b) Non Ideal Detonation in Combustible Gaseous Mixtures with Reactive Solid Particles. In: *Dynamic Structure of Detonation in Gaseous and Dispersed Media*. Kluwer Academic Publishers, pp.255–266
- Voronin DV, Zhdan SA (1984) Calculation of Heterogeneous Detonation Initiation for a Hydrogen-Oxygen Mixture in an Explosion Tube. *Fizika gorenia i vzryva* 20:461–465
- Zel'dovich YaB, Kompaneets AS (1960) *Theory of Detonations*. Academic Press, New York
- Zel'dovich YaB, Borisov AA, Gel'fand BE, Frolov S, Maikov AE (1988) Nonideal Detonation Waves in Rough Tubes. *Dynamics of Explosions*, AIAA Progress in Astronautics and Aeronautics, AIAA, NY 114:211–231